Journal of Materials Chemistry

Cite this: DOI: 10.1039/c2jm32056h

www.rsc.org/materials

PAPER

Harnessing Hansen solubility parameters to predict organogel formation

J. Gao, S. Wu and M. A. Rogers*

Received 2nd April 2012, Accepted 9th May 2012
DOI: 10.1039/c2jm32056h

Hansen solubility parameters predict the capacity of molecular gels to form in a vast array of organic solvents. The prediction ability for 12-hydroxystearic acid is closely associated with the hydrogen-bonding Hansen solubility parameter (δ_h). Solvents with a hydrogen-bonding Hansen solubility parameter less than 4.7 $MPa^{1/2}$ produce clear organogels, opaque organogel formed between $4.7 < \delta_h < 5.1$ $MPa^{1/2}$ and solutions remained when the hydrogen-bonding Hansen solubility parameter is greater than 5.1 $MPa^{1/2}$. Furthermore, the critical gelator concentration is linearly correlated with the hydrogen-bonding Hansen solubility parameter. Solvents with the same functional group, which varied only by chain length, have correlations between the static relative permittivity, Hansen solubility parameter, dispersive HSP, polar HSP and hydrogen-bonding HSP and the critical gelator concentration.

Introduction

Organogels are thermal reversible quasi-solid materials comprised mainly of organic liquids that undergo spontaneous formation of self-assembled fibrillar networks (SAFiNs).[1–3] The non-covalent interactions within these small molecules are capable of structuring fluids, preventing flow and improving the mechanical properties of some solids.[4,5] Numerous practical applications of organogels are being investigated pertaining to photovoltaics,[6] light harvesting,[7] templating reactions,[7] controlled drug release,[8] and reversible photoisomerization.[9]

SAFiNs, in organic solvents, require a meticulous balance between contrasting parameters including solubility and those intermolecular forces that control epitaxial growth into axially symmetric elongated aggregates.[2,10,11] The precise ratio of gelator–gelator interactions to gelator–solvent interactions is established to play a central role in the formation of an organogel; however, the direct effects of solvent on the physical properties are not well understood.[9,12] As solvent–gelator interactions increase the likelihood of directional gelator–gelator interactions decrease leading to thicker fibers.[9,13] In general, optimal gelation is achieved when the solvent and gelator are unable to form intermolecular hydrogen-bonds and the SAFiN is comprised of thin entangled fibers.[13] Typically, the intermolecular forces that drive aggregation are non-covalent in nature and include hydrogen-bonding,[14–17] π–π stacking, dipole–dipole,[18,19] and London dispersion forces;[20] however, the vast majority of reported organogelators are driven to spontaneously self-assemble by hydrogen-bonding.[9,21]

Due to the interplay between solvent and gelator, numerous attempts have been made to correlate solvent parameters to gelation ability.[11,22] The most promising technique was recently presented by Raynal and Bouteiller where they performed a meta-analysis, applying the Hansen solubility parameter to numerous LMOGs evaluating gelation behavior.[22] Their meta-analysis revealed that the solvents which gelled had similar Hanson solubility parameters (HSP) with only a few exceptions.[22] Numerous other measures of solubility have been applied to individual organogels which include dielectric constants,[23,24] Hildebrand solubility parameters[22] and the aforementioned HSPs.[22,24,25] Solubility parameters, although a new tool for organogels, have been well established for polymers, co-polymers, and systems employing multi-component solvents.[26–28] From an industrial perspective, understanding the interactions between solvents and gelating molecules is of utmost importance.

Hildebrand solubility parameters are governed by the free energy of mixing of the gelator and the solvent:

$$\Delta G_m = \Delta H_m - T\Delta S_m \quad (1)$$

where ΔG_m is the Gibbs free energy change during mixing, ΔH_m is the change in enthalpy during mixing, T is the absolute temperature and ΔS_m is the entropy change during mixing. It is assumed, in polymer physics, that the dissolution of the polymer is accompanied by a minor increase in the entropy, and the enthalpy is the deciding factor in the Gibbs free energy change. Therefore, the Hildebrand solubility parameter proposed in two seminal papers by Hildebrand and Scott[29] and Scatchard[30] relies solely on the enthalpy term:

$$\Delta H_m = V\left(\left[\frac{\Delta E_1^v}{V_1}\right]^{1/2} - \left[\frac{\Delta E_2^v}{V_2}\right]^{1/2}\right)^2 \phi_1\phi_2 \quad (2)$$

School of Environmental and Biological Sciences, Department of Food Science, Rutgers University, The State University of New Jersey, New Brunswick, NJ 08901, USA. E-mail: rogers@AESOP.Rutgers.edu

where V is the volume of the mixture, ΔE_i^v is the energy of vaporization of species i, V_i is the molar volume of species i and φ_i is the volume fraction of i in the mixture. Under isothermal vaporization of the saturated liquid, the cohesive energy density (ΔE_i^v) is the energy of vaporization per cm^3 which corresponds to the Hildebrand parameter δ_i.[26]

$$\delta_i = \left(\frac{\Delta E_i^v}{V_i}\right)^{1/2} \quad (3)$$

The HSP decomposes the cohesive energy density according to the dispersive interactions (δ_d), polar interactions (δ_p), and hydrogen-bonding interactions (δ_h).[26] It has been shown for solvents (j) that are capable of being gelled tend to cluster in a particular region of Hansen space (R).

$$R_{ij} = \left(4\left(\delta_{di} - \delta_{dj}^s\right)^2 + \left(\delta_{pi} - \delta_{pj}^s\right)^2 + \left(\delta_{hi} - \delta_{hj}^s\right)^2\right)^{1/2} \quad (4)$$

The objective of this manuscript is to scrutinize these parameters for a much wider class of solvents and to observe if significant trends exist that may correlate the individual HSPs to the critical gelator concentration.

Methods

Materials

Several classes of organic solvents were sub-divided into solvents capable of hydrogen-bonding, apolar and polar solvents (Table 1). The selection criteria for solvents were maintained as simply as possible with the aliphatic chain being linear, saturated, the functional group located in the primary position and the solvent must be in a liquid state between 10 and 30 °C. The only exceptions to these selection criteria were the ethers and ketones where the functional group was located in the exact middle of the molecule. Apolar solvents included aliphatics (pentane, hexane, heptane, octane, nonane, decane, dodecane, tetradecane), cycloalkanes (cyclopentane, cyclohexane, cyclooctane) and methyl halides (carbon tetrachloride, dichloromethane and chloroform). Polar solvents were subdivided into four categories: aldehydes (hexanal, octanal, nonanal and decanal), ketones (2-propone, 3-pentone, 4-nonanone, and 6-undecanone), ethers (diethyl ether, dipropyl ether, dibutyl ether and dipentyl ether) and nitriles (ethanenitrile, propanenitrile, pentanenitrile, and hexanenitrile). Hydrogen-bonding solvents were also divided into four groups, alcohols (1-butanol, 1-pentanol, 1-hexanal, 1-heptanol, 1-octanol, 1-nonanol, and 1-decanol), carboxylic acids (1-propanoic acid, 1-butanoic acid, 1-pentanoic acid, 1-hexanoic acid, 1-heptanoic acid, 1-octanoic acid, and 1-nonanoic acid), thiols (1-pentanethiol, 1-hexanethiol, 1-heptanethiol, and 1-octanethiol) and amines (1-butamine, 1-pentanamine, 1-hexamine, and 1-octanamine). All solvents and R-12-hydroxystearic acid (12HSA) were obtained from Sigma-Aldrich (Cherry Hill, NJ, USA) with purity greater than 0.95%.

Methods

Gel test. 12HSA was dispersed in each solvent at varying concentrations not exceeding 3 wt%, heated to 100 °C for 20 min, and stored for 24 hours at 20 °C; the vial was inverted for 1 hour and if the material did not flow it was considered to be gelled.

Solubility parameters. Dielectric constants were obtain from literature and were reported between 20 and 25 °C.[31] HSPs were obtained from literature[26] or were calculated from group contribution methods (GCMs), which is a widely accepted technique for approximating HSPs.[32–35] It is assumed that the functional groups' contribution to the cohesive energy density are additive which is true when one polar or hydrogen-bonding functional group is present.[26] Hoftyzer and van Krevelen's method to calculate HSPs were estimated using the following equations:[36]

$$\delta_d = \frac{\sum F_{di}}{V} \quad (5)$$

$$\delta_p = \frac{\sqrt{\sum F_{pi}^2}}{V} \quad (6)$$

$$\delta_h = \sqrt{\frac{\sum E_{hi}}{V}} \quad (7)$$

$$\delta_t = \left(\delta_p^2 + \delta_d^2 + \delta_h^2\right)^{\frac{1}{2}} \quad (8)$$

where δ_d is the dispersive HSP, δ_p is the polar HSP, δ_h is the hydrogen-bonding HSP, δ_t is the HSP, F_{di} is the dispersive component of the group contribution, F_{pi} is the polar component of the group contribution, E_{hi} is the hydrogen-bonding component of the group contribution and V is the molar volume.

Results and discussion

The ability to predict gelation behavior of organogels has been elusive due to the meticulous balance of contrasting parameters including solubility and the intermolecular forces controlling epitaxial growth. The solubility parameters, of the selected organic solvents, cover a vast breadth of static relative permittivities (1.82 to 37.5) (Table 1) as well as a large portion of Hansen space (Table 1 and Fig. 1). Due to the apolar nature of the solvents, the dispersive component of Hansen space is restricted, even though almost all of solvents fall within a narrow range of dispersive components ($14 < \delta_d < 20$).[27] Typically, if the solvent has a dispersive component below 14 MPa$^{1/2}$ it is in the gaseous state at atmospheric pressure and above 20 MPa$^{1/2}$ the solvent is a solid at 20 to 30 °C. The dispersive component of HSP is linearly correlated to the carbon length, while the polar and hydrogen-bonding HSP are inversely correlated.

For the 56 tested solvents, 32 are capable of forming organogels at concentrations below 3 wt%. An increase in the solvent aliphatic chain length increases the likelihood that a molecular gel will develop. However, beyond this there is no clear correlation between solvent type and the ability to gel, with the exception that neither alcohols nor carboxylic acids form molecular gels.

In an attempt to develop predicative tools to determine which solvents are immobilized by 12HSA, the individual HSPs, total HSP and static relative permittivity are examined as a function of critical gelator concentration (CGC) (Fig. 2). Solvents that

Table 1 Static relative permittivities (ε_r) obtained at 20 °C,[31] Hansen solubility parameters estimated using the groups contributions methods,[26] and distance in Hansen space from 12-hydroxysteaic acid (δ_d = 16.59 MPa$^{1/2}$, δ_p = 2.86 MPa$^{1/2}$, δ_h = 6.77 MPa$^{1/2}$), critical gelator concentration and appearance of 12HSA in various solvents

		ε_r	δ_T	δ_d	δ_p	δ_h	R_{ij}	CCG	
Organic solvent	Chemical structure	Unitless	MPa$^{1/2}$	MPa$^{1/2}$	MPa$^{1/2}$	MPa$^{1/2}$	MPa$^{1/2}$	wt%	State
Apolar									
Pentane	$CH_3(CH_2)_3CH_3$	1.82	14.90	14.90	0.00	0.00	9.11	0.5	Clear
Hexane	$CH_3(CH_2)_4CH_3$	1.89	14.90	15.30	0.00	0.00	9.11	0.4	Clear
Heptane	$CH_3(CH_2)_5CH_3$	1.91	15.30	15.50	0.00	0.00	8.66	0.3	Clear
Octane	$CH_3(CH_2)_6CH_3$	1.95	15.50	15.70	0.00	0.00	8.45	0.3	Clear
Nonane	$CH_3(CH_2)_7CH_3$	1.99	15.70	15.70	0.00	0.00	8.26	0.25	Clear
Decane	$CH_3(CH_2)_8CH_3$	2.00	15.70	16.00	0.00	0.00	8.26	0.2	Clear
Dodecane	$CH_3(CH_2)_{10}CH_3$	2.04	16.00	16.20	0.00	0.00	8.01	0.2	Clear
Tetradecane	$CH_3(CH_2)_{12}CH_3$	2.06	16.20	16.40	0.00	1.80	7.86	0.2	Clear
Cyclopentane	C_5H_{10}	1.96	16.50	16.80	0.00	0.20	6.21	0.5	Clear
Cyclohexane	C_6H_{12}	2.01	16.80	17.50	0.00	0.00	7.34	0.4	Clear
Cyclooctane	C_8H_{16}	2.11	17.50	17.70	0.00	0.00	7.35	0.4	Clear
Dichloromethane	CH_2Cl_2	8.51	20.23	17.80	3.10	5.70	3.69	2.5	Clear
Chloroform	$CHCl_3$	4.81	18.94	18.20	6.30	6.20	1.17	N/A	No gel
CCl_4	CCl_4	2.24	19.64	17.80	8.30	0.60	8.23	0.4	Clear
Polar									
Hexanal	$CH_3(CH_2)_4CHO$	9.50	18.32	15.90	7.40	5.30	5.85	N/A	No gel
Octanal	$CH_3(CH_2)_6CHO$	8.60	17.75	16.10	5.80	4.70	4.67	2.8	Opaque
Nonanal	$CH_3(CH_2)_7CHO$	7.60	17.62	16.20	5.28	4.50	4.33	2.5	Opaque
Decanal	$CH_3(CH_2)_8CHO$	6.80	17.53	16.30	4.80	4.30	4.06	1.6	Opaque
2-Propone	$CH_3(CHO)CH_3$	17.00	19.94	15.50	10.40	7.00	2.65	N/A	No gel
3-Pentone	$CH_3CH_2(CHO)CH_2CH_3$	11.20	18.15	15.80	7.60	4.70	2.17	N/A	No gel
4-Heptone	$CH_3(CH_2)_2(CHO)(CH_2)_2CH_3$	10.60	17.50	15.80	5.70	4.90	2.21	N/A	No gel
5-Nonanone	$CH_3(CH_2)_3(CHO)(CH_2)_3CH_3$	8.30	17.25	16.00	4.70	4.40	2.10	2.1	Clear
6-Undecanone	$CH_3(CH_2)_4(CHO)(CH_2)_4CH_3$	8.00	17.21	16.10	4.40	4.20	2.05	1.6	Clear
Diethyl ether	$CH_3CH_2OCH_2CH_3$	4.33	15.64	14.50	2.90	5.10	6.40	N/A	No gel
Dipropyl ether	$CH_3(CH_2)_2O(CH_2)_2CH_3$	3.34	16.10	15.10	4.20	3.70	6.00	2.2	Clear
Dibutyl ether	$CH_3(CH_2)_3O(CH_2)_3CH_3$	3.22	16.13	15.20	3.40	4.20	5.45	1.5	Clear
Dipentyl ether	$CH_3(CH_2)_4O(CH_2)_4CH_3$	3.10	16.00	15.30	3.30	4.40	5.30	1.4	Clear
Ethanenitrile	CH_3CN	37.50	24.40	15.30	18.00	6.10	15.83	2.3	Opaque
Propanenitrile	CH_3CH_2CN	27.20	21.65	15.30	14.30	5.50	12.39	2.3	Opaque
Butanenitrile	$CH_3(CH_2)_2CN$	20.30	20.40	15.30	12.50	5.10	10.80	2.1	Clear
Hexanenitrile	$CH_3(CH_2)_4CN$	17.26	18.56	15.30	9.50	4.50	8.38	1.9	Clear
Octanenitrile	$CH_3(CH_2)_6CN$	14.70	17.56	15.30	7.60	4.10	7.11	1.5	Clear
Nonanenitrile	$CH_3(CH_2)_7CN$	14.00	17.00	15.30	6.60	3.80	6.62	0.9	Clear
H-Bonding									
1-Butanol	$CH_3(CH_2)_3OH$	17.92	23.20	16.00	5.70	15.80	3.97	N/A	No gel
1-Pentanol	$CH_3(CH_2)_4OH$	14.50	21.93	15.90	5.90	13.90	3.73	N/A	No gel
1-Hexanol	$CH_3(CH_2)_5OH$	13.02	21.04	15.90	5.80	12.50	3.54	N/A	No gel
1-Heptanol	$CH_3(CH_2)_6OH$	11.48	20.52	16.00	5.30	11.70	3.42	N/A	No gel
1-Octanol	$CH_3(CH_2)_7OH$	9.75	21.01	17.00	3.30	11.90	3.45	N/A	No gel
1-Nonanol	$CH_3(CH_2)_8OH$	8.58	20.44	16.80	4.80	10.60	3.26	N/A	No gel
1-Decanol	$CH_3(CH_2)_9OH$	7.70	19.44	16.00	4.70	10.00	3.16	N/A	No gel
1-Propanoic acid	CH_3CH_2COOH	3.20	19.95	14.70	5.30	12.40	8.43	N/A	No gel
1-Butanoic acid	$CH_3(CH_2)_2COOH$	2.88	19.11	14.80	5.00	11.00	7.32	N/A	No gel
1-Pentanoic acid	$CH_3(CH_2)_3COOH$	2.66	18.65	15.00	4.10	10.30	6.39	N/A	No gel
1-Hexanoic acid	$CH_3(CH_2)_4COOH$	2.82	18.17	15.00	4.10	9.40	5.94	N/A	No gel
1-Heptanoic acid	$CH_3(CH_2)_5COOH$	3.03	18.48	15.80	3.80	8.80	4.22	N/A	No gel
1-Octanoic acid	$CH_3(CH_2)_6COOH$	2.82	17.50	15.10	3.30	8.20	5.20	N/A	No gel
1-Nonanoic acid	$CH_3(CH_2)_7COOH$	1.72	18.05	16.00	3.00	7.80	3.35	N/A	No gel
1-Pentanethiol	$CH_3(CH_2)_3CHSH$	4.67	17.45	16.30	4.60	4.20	2.05	0.5	Clear
1-Hexanethiol	$CH_3(CH_2)_4CHSH$	4.34	17.25	16.30	4.10	3.90	1.97	0.45	Clear
1-Heptanethiol	$CH_3(CH_2)_5CHSH$	4.11	17.17	16.35	3.70	3.70	1.92	0.45	Clear
1-Octanethiol	$CH_3(CH_2)_6CHSH$	3.95	17.09	16.40	3.30	3.50	1.87	0.4	Clear
1-Decanethiol	$CH_3(CH_2)_8CHSH$	3.84	17.02	16.45	2.90	3.30	1.80	0.3	Clear
1-Butanamine	$CH_3(CH_2)_3NH_2$	4.90	17.78	14.95	4.50	8.50	2.92	N/A	No gel
1-Pentanamine	$CH_3(CH_2)_4NH_2$	5.36	17.56	15.20	3.87	7.90	2.81	N/A	No gel
1-Hexanamine	$CH_3(CH_2)_5NH_2$	3.53	17.46	15.40	3.40	7.50	2.74	N/A	No gel
1-Heptylamine	$CH_3(CH_2)_6NH_2$	3.42	17.42	15.50	3.10	7.30	2.70	N/A	No gel
1-Octanamine	$CH_3(CH_2)_7NH_2$	3.30	17.37	15.60	2.80	7.10	2.66	N/A	No gel

remained as a solution, at concentrations less than 3 wt%, are represented graphically with a CGC of 10. Overall, neither the static relative permittivity, dispersive nor the polar HSP are able to predict gelation ability of 12HSA in the various solvents (Fig. 2A, B and E). It is not astonishing that the static relative permittivity is incapable of predicting gelation capacity since it

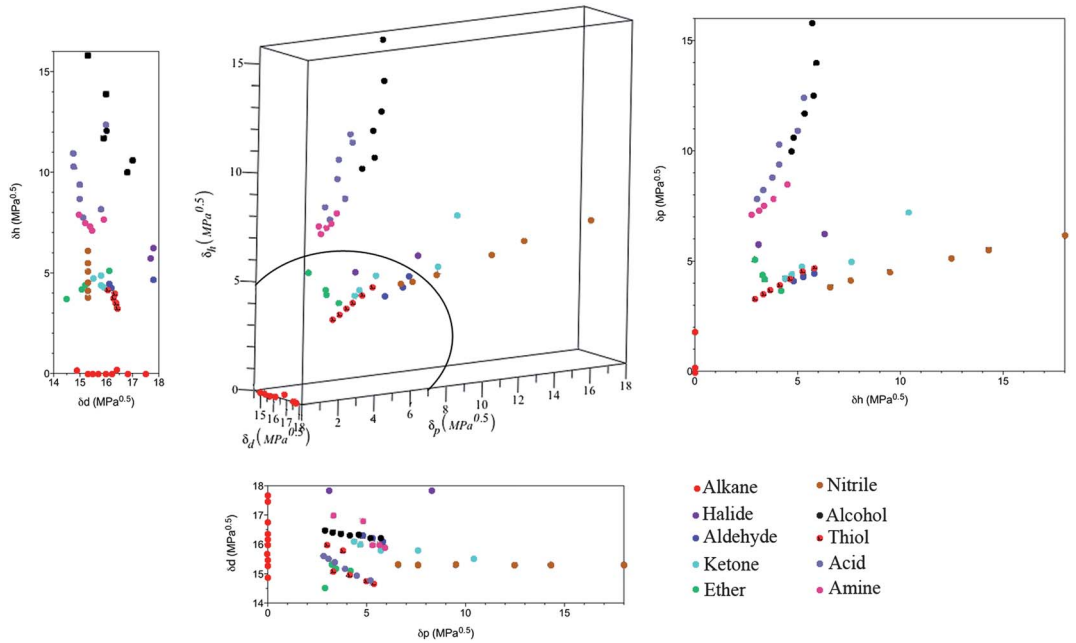

Fig. 1 Hansen space of the selected solvents categorized by functional group located in the primary position with varying aliphatic chain lengths. Lower left area was the region of Hansen space where solvents gelled.

does not account for the complex interactions involving functional groups between the solvent and gelator.[11] Interestingly, the hydrogen-bonding HSP establishes a distinct relationship between gelating capacity and CGC (Fig. 2C). Very convincing trends between the hydrogen-bonding HSP and the ability to form clear organogels (δ_h < 4.7 MPa$^{0.5}$), opaque organogel (4.7 < δ_h < 5.1 MPa$^{0.5}$) and solutions (δ_h > 5.1 MPa$^{0.5}$) are observed. The turbidity or transparency of an organogel has been correlated to the cross-sectional thickness of the crystalline aggregates, number of junction zones capable of diffracting light, and the number of crystalline aggregates within the self-assembled network.[37–39] Zhu and Dordick reported that solvent–gelator interactions weaken gelator–gelator intermolecular hydrogen bonding interactions and result in thicker crystalline fibers.[13] Further increasing the solvent–gelator interactions cause the fibrous structures to be lost resulting in the complete absence of crystal structure.[13]

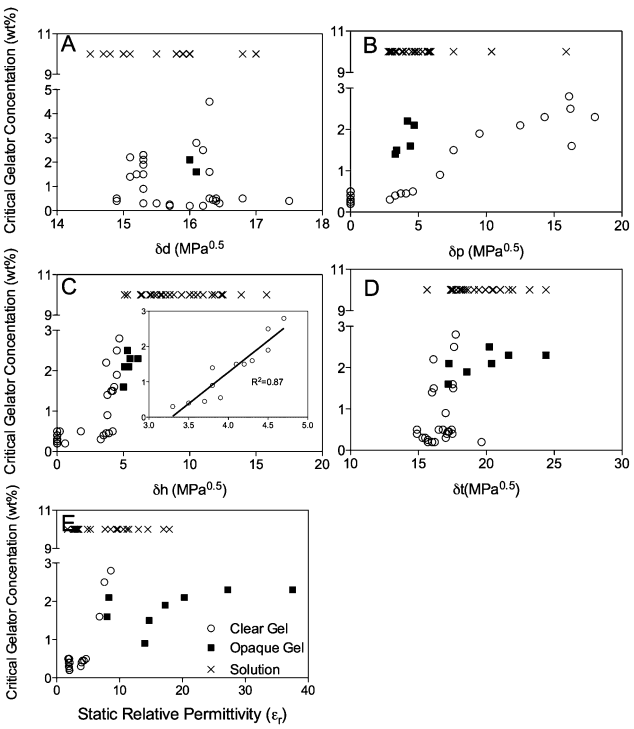

Fig. 2 Critical gelator concentration as determined using the inverted vial test, as a function of the: dispersive Hansen solubility parameter (δ_d) (A); polar Hansen solubility parameter (δ_p) (B); hydrogen-bonding Hansen solubility parameter (δ_h) (C); total Hansen solubility parameter (δ_t) (D); and the static relative permittivity (ε_r) (E). Solvents which did not gel were graphically represented with a CGC of 10.

The intermolecular interactions required for 12HSA to form molecular gels has been very well established.[11,14,15,40–44] 12HSA's cross-sectional fiber width is a multiple of the carboxylic acid dimer length while longitudinal growth occurs *via* hydrogen-bonding between hydroxyl group at position 12. Hence, if the hydrogen-bonding component is too strong then it will interfere with the formation of gelator–gelator intermolecular hydrogen-bonding thus disrupting gel formation. For 12HSA this occurs at a hydrogen-bonding HSP greater than 4.7 MPa$^{1/2}$ (Fig. 2). The CGC also scales with hydrogen-bonding HSP (Fig. 2C inset). This confirms that as the solvent–gelator interactions increases, more 12HSA is required to form an organogel. The overall HSP is also useful in distinguishing between which solvents will develop translucent fibrillar networks *versus* solutions (Fig. 2D). However, there is an overlap between the HSPs which form opaque gels (very weak structures which break down under force) and which solvents remain as solutions. Thus, irrespective of the type of solvent, the individual hydrogen-bonding and total HSP are useful predicative tools for the gelation behavior of molecular gels.

In order to better assess the effect of solvent composition on gelation capacity, Teas diagrams are used to examine correlations between gelation ability and solvent HSP parameters (Fig. 3). Individual HSP are converted to an average value by dividing each parameter by the sum of the three HSPs:

$$\Xi_d = \frac{\delta_d}{\delta_d + \delta_h + \delta_p} \quad (9)$$

$$\Xi_p = \frac{\delta_p}{\delta_d + \delta_h + \delta_p} \quad (10)$$

$$\Xi_h = \frac{\delta_h}{\delta_d + \delta_h + \delta_p} \quad (11)$$

where Ξ is the percent fraction of the individual HSP component. The Teas plot shows a clustering of solvents capable of gelling and another region that remain as solution (Fig. 3). Since we are working with apolar solvents, the dispersive parameter is greater than 50% for all solvents tested. The polar component varies from 50% to as low as 10% and does not influence gelation behavior. However, it is extremely clear that the hydrogen-bonding HSP cannot exceed 18% of the total HSP or the system will not form an organogel. Recent work with dicholesterol-linked azobenzene organogels suggests that as the combination of solvents (*i.e.*, greater concentrations of methanol) and gelator move further apart in Hansen space then they interact less becoming more efficient gelators.[9] Since the solvents, which gel cluster in a specific region on the Teas plot, it is reasonable to assume that the role of Hansen space is important in predicting gel formation.

One distinction between Wu *et al.*'s,[9] work and ours is that they modified solvent parameters by adjusting the concentration of two mixed solvents while our study examined single solvents with different functional groups and varying alkane chain lengths. The Hansen solubility parameter for 12HSA was calculated using the group contribution method and the distance in Hansen space was calculated using eqn (4). The distance in Hansen space was not the only factor when deciding if a solvent would form an organogel (Fig. 4). Along with the distance in Hansen space, the overall HSP was needed to predict organogel formation. This indicates that there is a limit to how close in Hansen space the solvent and gelator may be (*i.e.*, if they are too close then the solvent–gelator interactions solubilize the gelator). However, the direction in Hansen space is crucial in determining the ability of the gelator to gel the solvent. It becomes clear that HSPs are very powerful tools when trying to understand and predict the likelihood of organogel formation.

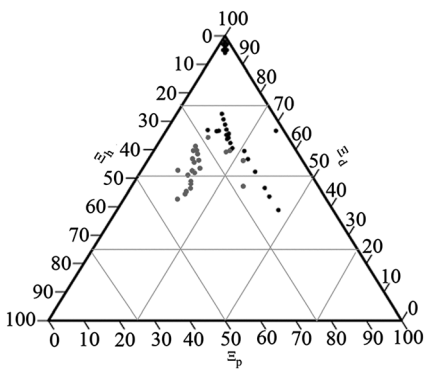

Fig. 3 Teas plot of calculated solubility parameters for 12-hydroxystearic acid in varying solvents. Black circles represent solvents that gelled and grey circles are solvents unable to gel.

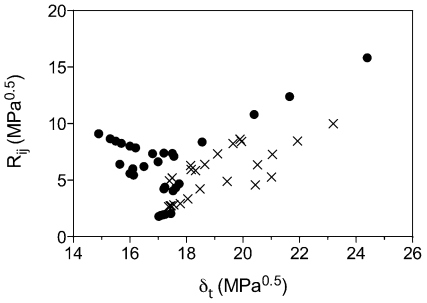

Fig. 4 Distance in Hansen space between the solvent and 12-hydroxystearic acid (δ_d = 17.59 MPa$^{1/2}$, δ_p = 2.86 MPa$^{1/2}$, δ_h = 6.77 MPa$^{1/2}$) *versus* the total Hansen solubility parameter (circles represent gelled solvent, × represent solutions).

In order to confirm that these trends were not specific to 12HSA, CGC reported by Abdallah and Weiss, were examined for ammonium bromide salts where nitrogen was covalently linked to four equal long alkyl chains (ranging from 12 to 18 carbons) (Fig. 5).[45] Neither the dispersive HSP nor the polar HSP (Fig. 5A and B) were correlated to the CGC. Similar to 12HSA, the CGC is constant below a critical value for the hydrogen-bonding HSP and total HSP. For ammonium bromide salts the hydrogen-bonding HSP is 6 and total HSP is 19 and above these values the CGC increases (Fig. 5C and D). It is also worth noting that the solvents used in Abdallah and Weiss's study (alkanes, benzene, CCl_4, styrene, methyl methacrylate and glycidyl methacrylate) were not the same as we selected for 12HSA suggesting that HSP universally apply to an even broader group of solvents then tested in this present study.

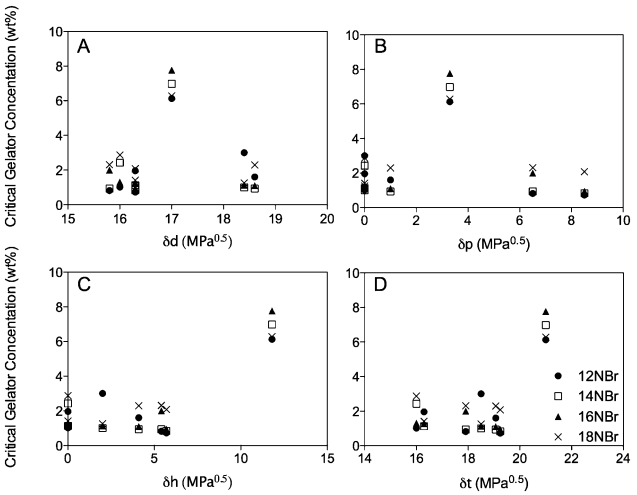

Fig. 5 Critical gelator concentrations for ammonium bromide salts: dispersive Hansen solubility parameter (δ_d) (A); polar Hansen solubility parameter (δ_p) (B); hydrogen-bonding Hansen solubility parameter (δ_h) (C); and total Hansen solubility parameter (δ_t) (D).

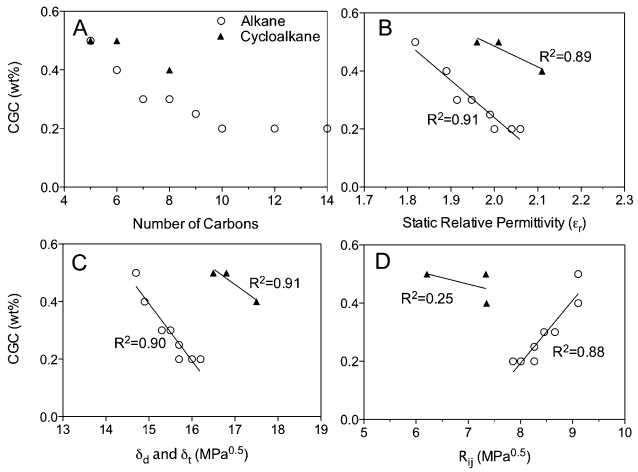

Fig. 6 Critical gelator concentration *versus* carbon number (A), static relative permittivity (B), Hansen solubility parameter and the dispersive component of the Hansen solubility parameter (C) and the distance in Hansen space (D) for alkanes.

Although the predictive nature of the HSP is much stronger than originally anticipated for the wide range of solvents. The parameter becomes even more powerful when observing the CGC as a function of the individual HSP within the individual classes of solvents. As the carbon length of the solvent increases, the static relative permittivity, the HSP and the dispersive component of the HSP increase while the distance in Hansen space decreases (Table 1). On the other hand, for polar and hydrogen-bonding solvents, as the chain length increases the static relativity permittivity, the hydrogen-bonding HSP and polar HSP decrease while the dispersive HSP increases (Table 1). As the chain length of the aliphatic solvents increase (*i.e.*, increased static relative permittivity) the CGC decreases (Fig. 6A and B). The HSP and dispersive HSP are inversely correlated to the critical gelator concentration while the distance in Hansen space is correlated linearly (Fig. 6C and D). Only three sets of polar solvents (*i.e.*, aldehydes, ethers, and nitriles) and one set of hydrogen-bonding solvents (*i.e.*, amines) could be observed for correlations between CGC and the solubility parameters due to a lack of samples which gelled. As the chain length increases for polar and hydrogen-bonding solvents, the CGC decreases (Fig. 7A and 8A). Furthermore, the CGC is inversely

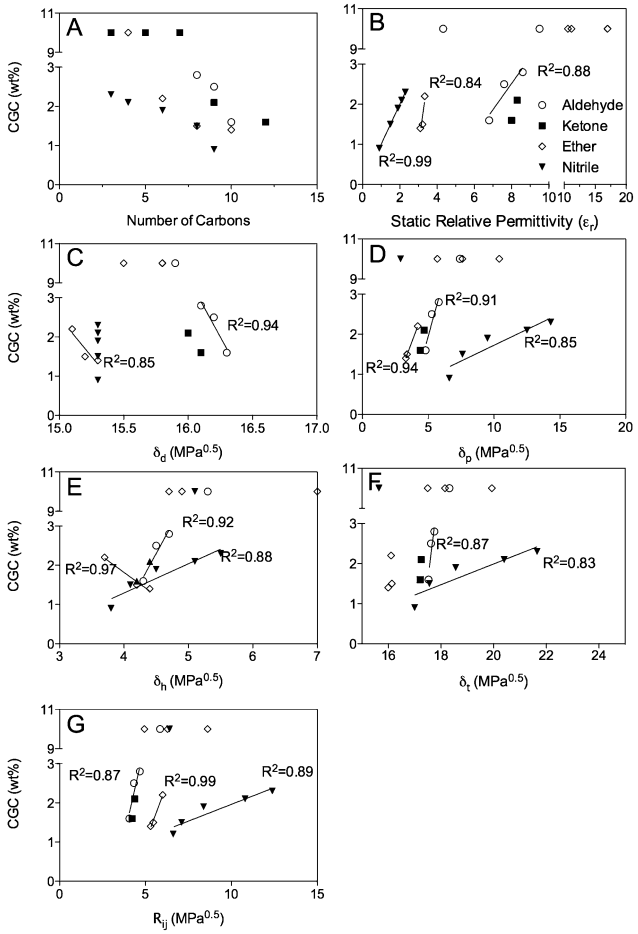

Fig. 7 Critical gelator concentration *versus* carbon number (A), static relative permittivity (B), the dispersive component of the HSP (C), the polar component of the HSP (D), the hydrogen-bonding component of the HSP (E), the total HSP (F) and the distance in Hansen space (G) for polar solvents.

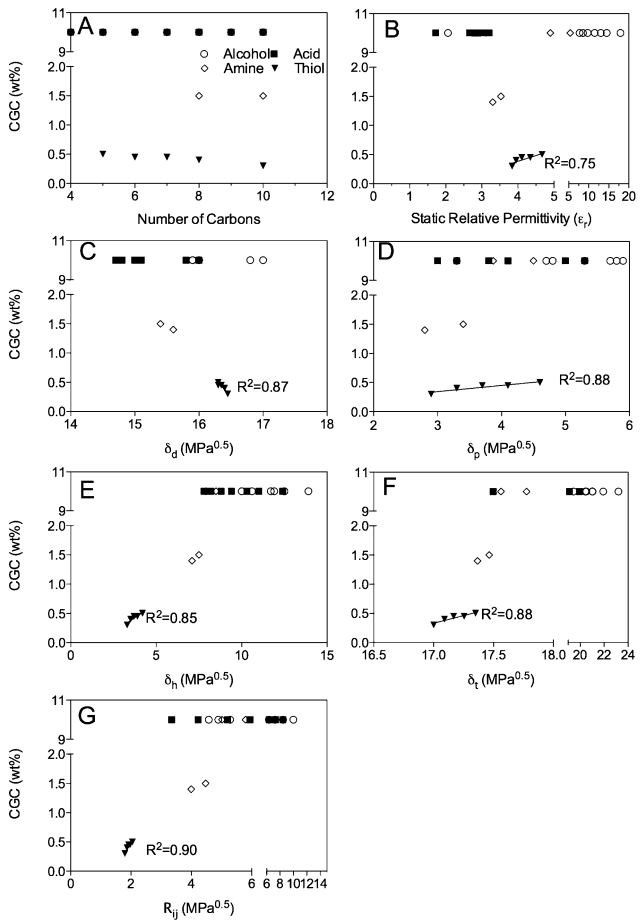

Fig. 8 Critical gelator concentration *versus* carbon number (A), static relative permittivity (B), the dispersive component of the HSP (C), the polar component of the HSP (D), the hydrogen-bonding component of the HSP (E), the total HSP (F) and the distance in Hansen space (G) for hydrogen bonding solvents.

proportional to the dispersive HSP, and proportional to the polar (Fig. 7D and 8D), hydrogen-bonding HSP (Fig. 6E and 7E), the HSP (Fig. 7F and 8F) and the distance in Hansen space (Fig. 7G and 8G). Upon closer examination of the hydrogen-bonding solvents, as the hydrogen-bonding strength of the primary functional group decreases (*i.e.*,–COOH > –COH > $–NH_2$ > –SH) the CGC decreases (Fig. 8A). Therefore, as the hydrogen-bonding strength of the solvent decreases, it is less likely to interfere with the dimerization and longitudinal of 12HSA.

Conclusions

Hansen solubility parameters are useful in predicating which solvents are immobilized using low molecular organogelators. The predication ability for 12-hydroxystearic acid is related to the hydrogen-bonding Hansen solubility parameter (*i.e.*, Hansen solubility parameter less than 4.7 $MPa^{1/2}$ produces clear organogels). CGC also scales as a function of the hydrogen-bonding HSPs. Solvents with the same functional group, which varied only by chain length, have linear correlations between static relative permittivity, HSP, dispersive HSP, polar HSA and hydrogen-bonding HSP and the CGC.

References

1 V. A. Mallia, P. D. Butler, B. Sarkar, K. T. Holman and R. G. Weiss, Reversible phase transitions within self-assembled fibrillar networks of (*R*)-18-(*n*-alkylamino)octadecan-7-ols in their carbon tetrachloride gels, *J. Am. Chem. Soc.*, 2011, **133**, 15045–15054.
2 R. G. Weiss and P. Terech, Introduction, in *Molecular Gels: Materials with Self-Assebled Fibrillar Networks*, ed. R. G. Weiss and P. Terech, Springer, Dordrecht, The Neatherlands, 2006, pp. 1–13.
3 M. George and R. G. Weiss, Molecular organogels. Soft matter comprised of low-molecular-mass organic gelators and organic liquids, *Acc. Chem. Res.*, 2006, **39**, 489–497.
4 M. Fahrländer, K. Fuchs, R. Mülhaupt and C. Friedrich, Linear and nonlinear rheological properties of self-assembling tectons in polypropylene matrices, *Macromolecules*, 2003, **36**, 3749–3757.
5 B. Isare, L. Petit, E. Bugnet, R. Vincent, L. Lapalu, P. Sautet and L. Bouteiller, The weak help the strong: low-molar-mass organogelators harden bitumen, *Langmuir*, 2009, **25**, 8400–8403.
6 W. Kubo, K. Murakoshi, T. Kitamura, S. Yodhida, M. Haruki, K. Hanabusa, H. Shirai, Y. Wada and S. Yanagida, Quasi-solid-state dye-sensitized TiO_2 solar cells: effective charge transport in mesoporous space filled with gel electrolytes containing iodide and iodine, *J. Phys. Chem. B*, 2001, **105**, 12809–12815.
7 K. Sugiyasu, N. Fujita and S. Shinkai, Visible-light-harvesting organogel composed of cholesterol-based perylene derivatives†, *Angew. Chem., Int. Ed.*, 2004, **43**, 1229–1233.
8 A. Friggeri, B. L. Feringa and J. van Esch, Entrapment and release of quinoline derivatives using a hydrogel of a low molecular weight gelator, *J. Controlled Release*, 2004, **97**, 241–248.
9 Y. Wu, S. Wu, G. Zou and Q. Zhang, Solvent effects on structure, photoresponse and speed of gelation of a dicholesterol-linked azobenzene organogel, *Soft Matter*, 2011, **7**, 9177–9183.
10 M. Suzuki, Y. Nakajima, M. Yumoto, M. Kimura, H. Shirai and K. Hanabusa, Effects of hydrogen bonding and van der Waals interactions on organogelation using designed low-molecular-weight gelators and gel formation at room temperature, *Langmuir*, 2003, **19**, 8622–8624.
11 M. A. Rogers and A. G. Marangoni, Solvent-modulated nucleation and crystallization kinetics of 12-hydroxystearic acid: a nonisothermal approach, *Langmuir*, 2009, **25**, 8556–8566.
12 A. R. Hirst, I. A. Coates, T. R. Boucheteau, J. F. Miravet, B. Escuder, V. Castelletto, I. W. Hamley and D. K. Smith, Low-molecular-weight gelators: elucidating the principles of gelation based on gelator solubility and a cooperative self-assembly model, *J. Am. Chem. Soc.*, 2008, **130**, 9113–9121.
13 G. Zhu and J. S. Dordick, Solvent effect on organogel formation by low molecular weight molecules, *Chem. Mater.*, 2006, **18**, 5988–5995.
14 T. Kuwahara, H. Nagase, T. Endo, H. Ueda and M. Nakagaki, Crystal structure of DL-12-hydroxystearic acid, *Chem. Lett.*, 1996, **25**, 435–436.
15 R. Lam, L. Quaroni, T. Pederson and M. A. Rogers, A molecular insight into the nature of crystallographic mismatches in self-assembled fibrillar networks under non-isothermal crystallization conditions, *Soft Matter*, 2010, **6**, 404–408.
16 J. L. Li, X. Y. Liu, R. Y. Wang and J. Y. Xiong, Arichitecture of a biocompatible supramolecular material by supersaturation-driven fabrication of its network, *J. Phys. Chem. B*, 2005, **109**, 24231–24235.
17 M. A. Rogers, A. Bot, R. S. H. Lam, T. Pedersen and T. May, Multicomponent hollow tubules formed using phytosterol and γ-oryzanol-based compounds: an understanding of their molecular embrace, *J. Phys. Chem. B*, 2010, **114**, 8278–8295.
18 T. Brotin, J. P. Devergne and F. Fages, Photostationary fluorescence emission and time resolved spectroscopy of symmetrically disubstituted anthracenes on the *meso* and side rings: the unusual behavior of the 1,4 derivative, *Photochem. Photobiol.*, 1992, **55**, 349–358.
19 P. Terech, I. Furman and R. G. Weiss, Structures of organogels based upon cholesteryl-4-(2-anthryloxy)butanoate, a highly efficient luminescing gelator – neutron and X-ray small-angle scattering investigations, *J. Phys. Chem.*, 1995, **99**, 9558–9566.
20 J. F. Toro-Vazquez, J. Morales-Rueda, V. A. Mallia and R. G. Weiss, Relationship between molecular structure and thermo-mechanical properties of Candelilla wax and amides derived from (*R*)-12-hydroxystearic acid as gelators of safflower oil, *Food Biophys.*, 2010, **5**, 193–202.
21 J. van Esch and B. L. Feringa, New functional materials based on self-assembling organogels: from serendipity towards design, *Angew. Chem., Int. Ed.*, 2000, **39**, 2263–2266.
22 M. Raynal and L. Bouteiller, Organogel formation rationalized by Hansen solubility parameters, *Chem. Commun.*, 2011, **47**, 8271–8273.
23 A. Aggeli, M. Bell, M. Boden, J. N. Keen, P. F. Knowles, T. C. B. McLeish, M. Pitkeatly and S. E. Radford, Responsive gels formed by the spontaneous self-assembly of peptides into polymeric β-sheet tapes, *Nature*, 1997, **386**, 259–262.
24 A. R. Hirst and D. K. Smith, Solvent effects on supramolecular gel-phase materials: two-component dendritic gel, *Langmuir*, 2004, **20**, 10851–10857.
25 K. Hanabusa, M. Matsumoto, M. Kimura, A. Kakehi and H. Shirai, Low molecular weight gelators for organic fluids: gelation using a family of cyclo(dipeptide)s, *J. Colloid Interface Sci.*, 2000, **224**, 231–244.
26 *Solubility Parameter Values*, ed. E. A. Grulke, John Wiley & Sons: New York, NewYork, 4th edn, 2005.
27 C. M. Hansen, *Hansen Solubility Parameters*, CRC Press, Boca Raton, FL, 2nd edn, 2007.
28 H. T. Ham, Y. S. Choi and I. J. Chung, An explanation of dispersion states of single-walled carbon nanotubes in solvents and aqueous surfactant solutions using solubility paramters, *J. Colloid Interface Sci.*, 2006, **286**, 216–223.
29 J. H. Hildebrand and R. L. Scott, *The Solubility of Nonelectrolytes*, Dover Publications, Reinhold, NY, 3rd edn, 1959.
30 G. Scatchard, Equilibrium in nonelectrolyte mixtures, *Chem. Rev.*, 1949, **44**, 7–35.
31 C. H. Wohlfahrt, Pure Liquids: References, in *Landolt-Börnstein – Group IV Physical Chemistry Numerical Data and Functional Relationships in Science and Technology*, ed. O. Madelung, Springer, 1991, vol. 6, Static Dielectric Constants of Pure Liquids and Binary Liquid Mixtures.
32 M. Jang, R. M. MKamens, K. B. Leach and M. R. Strommen, A thermodynamic approach using group contribution methods to model the partitioning of semivolatile organic compounds on atmospheric particulate matter, *Environ. Sci. Technol.*, 1997, **31**, 2805–2811.
33 R. F. Fedors, A method for estimating both the solubility parameters and molar volumes of liquids, *Polym. Eng. Sci.*, 1974, **14**, 147–154.

34 T. Lindvig, M. L. Michelsen and G. M. Kontogeorgis, A Flory–Huggins model based on the Hansen solubility parameters, *Fluid Phase Equilib.*, 2002, **203**, 247–260.
35 D. W. van Krevelen and P. J. Hoftyzer, Practical evaluation of the [n]–M relation, *J. Appl. Polym. Sci.*, 1967, **11**, 2189–2200.
36 D. W. van Krevelen, *Properties of Polymers*, Elsevier, New York, NY, 3rd edn, 1990.
37 P. Terech, D. Pasquier, V. Bordas and C. Rossat, Rheological properties and structural correlations in molecular gels, *Langmuir*, 2000, **16**, 4485–4494.
38 T. Tamura and M. Ichikawa, Effect of lecithin on organogel formation of 12-hydroxystearic acid, *J. Am. Oil Chem. Soc.*, 1997, **74**, 491–495.
39 S. Abraham, Y. Lan, R. S. H. Lam, D. A. S. Grahame, J. J. H. Kim, R. G. Weiss and M. A. Rogers, Influence of positional isomers on the macroscale and nanoscale architectures of aggregates of racemic hydroxyoctadecanoic acids in their molecular gel, dispersion, and solid states, *Langmuir*, 2012, 4955–4964.
40 M. A. Rogers and A. G. Marangoni, Non-isothermal nucleation and crystallization of 12-hydroxystearic acid in vegetable oils, *Cryst. Growth Des.*, 2008, **8**, 4596–4601.
41 M. A. Rogers, A. J. Wright and A. G. Marangoni, Engineering the oil binding capacity and crystallinity of self-assembled fibrillar networks of 12-hydroxystearic acid in edible oils, *Soft Matter*, 2008, **4**, 1483–1490.
42 M. A. Rogers, A. J. Wright and A. G. Marangoni, Nanostructuring fiber morphology and solvent inclusions in 12-hydroxystearic acid/canola oil organogels, *Curr. Opin. Colloid Interface Sci.*, 2009, **14**, 223.
43 P. Terech, 12-D-Hydroxyoctadecanoic acid organogels – a small-angle neutron-scattering study, *J. Phys. II*, 1992, **2**, 2181–2195.
44 P. Terech, V. Rodriguez, J. D. Barnes and G. B. McKenna, Organogels and areogels of racemic and chiral 12-hydroxyoctadecanoic acid, *Langmuir*, 1994, **10**, 3406–3418.
45 A. J. Abdallah and R. G. Weiss, Organogels and low molecular mass organic gelators, *Adv. Mater.*, 2000, **12**, 1237–1247.